

Electronic-structure calculations of the Cr/GaAs(001) interface

M. C. Muñoz and M. P. López Sancho

*Instituto de Ciencia de Materiales, Madrid Consejo Superior de Investigaciones Científicas,
Calle Serrano 144, E-28006 Madrid, Spain*

(Received 7 August 1989; revised manuscript received 27 November 1989)

The electronic structure of the Cr/GaAs(001) interfaces, both Cr-Ga and Cr-As, are calculated within the surface Green-function matching formalism. The Hamiltonian used is of the tight-binding type with first- and second-order interactions. A basis of one s and three p atomic orbitals for GaAs and five d orbitals for Cr is employed; the interface parameters are taken as the geometric mean of the constituent material matrix elements. Metallic character and enhancement of the Cr magnetic moment at both interfaces, although lower than that of the Cr(001) surface, is found. The local densities of states present interface-induced effects in the energy range of the Cr d -band width, which are important at the first three layers of the GaAs and at the interface layer of the Cr semi-infinite crystals.

I. INTRODUCTION

There is considerable interest in the study of boundary regions, since they are related to the development of microelectronic devices, synthesis of new materials, and catalysis. A great deal of experimental and theoretical work has been done to understand and control the properties of interfaces.¹ Metal-semiconductor interfaces are among the most studied because they play a main role in device performance and determine important device features.²⁻⁵ In particular, transition-metal-III-V-semiconductor interfaces have received much attention recently due to their technological importance, but many aspects of them are still not well known.⁶⁻⁹ This paper is a study of the electronic properties of the Cr/GaAs(001) heterojunction.

Chromium is a body-centered-cubic (bcc) $3d$ transition metal with intriguing magnetic properties. The Cr(001) surface presents an induced ferromagnetism with a very high magnetic moment, $2.49\mu_B$, while antiferromagnetic coupling is observed in the bulk, with a magnetization, at maximum, of $0.59\mu_B$. These differences between bulk- and surface-electronic properties made the Cr(001) surface very interesting to examine in terms of its behavior in the presence of a dissimilar neighbor.⁶⁻¹⁸ Works about the possible existence of superconductivity in Au/Cr/Au(001) sandwiches¹⁹ point out the complexity of this behavior. Therefore, Cr/GaAs(001), which is a nearly lattice-matched interface, offers a good opportunity for investigating magnetic properties at interfaces. Cr/GaAs is a prototypical system of reactive overlayers on a III-V compound semiconductor, so it is of both technological and fundamental interest. Xu *et al.*,¹⁸ using high-resolution x-ray photoemission, have studied the temperature-dependent evolution of the Cr/GaAs(100) interface, reporting that heating promotes substrate disruption. It seems that Cr reacts with As to form an arsenide and releases Ga into the growing metal overlayer. Previous studies on the Cr/GaAs(110) interface^{7,17} have

pointed out that Cr atoms interact weakly with GaAs(110) for low coverages, and that substrate disruption and reactive interdiffusion start only at a coverage of 2 \AA , when Cr-As and Cr-Ga bonds are formed.

We have investigated the two possible Cr-Ga and Cr-As interfaces of the ideal Cr/GaAs(001) heterojunction, unrelaxed and abrupt. Their electronic structures have been calculated within the surface Green-function matching formalism (SGFM),^{20,21} taking advantage of the transfer-matrix approach.^{22,23} This method provides an exact solution for the interface Green function, since it takes into account the true two semi-infinite media forming the interface, avoiding the undesirable slab effects. The outline of this paper is as follows. The theoretical model and method of calculation are briefly described in Sec. II, pointing out the peculiarities of the present case. In Sec. III results are discussed, and finally some conclusions are summarized in Sec. IV.

II. METHOD

The surface Green-function matching approach provides a framework of exact theory within which the Green function (GF) of layered structures such as surfaces, interfaces, quantum wells, and superlattices can be calculated. The method combines elements of scattering theory with the treatment of the boundary conditions, to give an exact analysis of the interface problem, within the context of the model Hamiltonian employed. The SGFM yields a procedure to construct the GF of the system in terms of the coupling interactions across the interface and the projections on the interface domain of the bulk Hamiltonians and GF's of the constituent crystals. This approach, which can be used with different one-electron Hamiltonian models, has been successfully employed with semiempirical tight-binding (TB) Hamiltonians, to describe the electronic properties of surfaces, interfaces, and superlattices of semiconductor materials.²⁰⁻²² The general formal theory for ideal and nonideal interfaces is described elsewhere;²¹ therefore only the main formulas

will be given here, as well as the modifications required by the magnetic nature of the Cr model.

Since two-dimensional periodicity is retained in the interface and \mathbf{k} parallel is a good quantum number, the system will be described in terms of principal layers. A principal layer may contain one or more atomic planes, and, by definition, is coupled only to its nearest-neighbor principal layers. Within the TB layer representation, the Hamiltonian H and the GF G are \mathbf{k} -dependent matrices, where \mathbf{k} is a vector of the two-dimensional Brillouin zone (BZ). An element of, for example, the G matrix, would be denoted $G_{\mathbf{n}\mathbf{n}'} = \langle \mathbf{n}, \alpha | G(\mathbf{k}) | \mathbf{n}', \alpha' \rangle$, where \mathbf{n} and \mathbf{n}' are layer indexes and α and α' stand for the orbitals. The \mathbf{k} dependence is understood henceforth.

In the present work an ideal interface is considered, defined as the coupling of two abruptly terminated semi-infinite crystals, keeping all the intra- and interatomic interactions unaltered. Thus, the interaction between principal layers \mathbf{n} and \mathbf{n}' is given by $H_{\mathbf{n}\mathbf{n}'}$ and, by definition of the principal layer $H_{\mathbf{n}\mathbf{n}'} = 0$ if $|\mathbf{n} - \mathbf{n}'|$ is greater than 1. Extension to the nonideal case is straightforward and has already been made.²¹ Now consider the ideal interface as the A/B bicrystal; the complete interface domain contains two principal layers—one belongs to the semi-infinite crystal A and the other to B . The SGFM method yields the following formula for the GF projection \mathbf{g}_I onto the interface domain:

$$\begin{aligned} I\mathbf{g}_I^{-1}I &= I_A(w - H_A P_A G_A \mathbf{g}_A^{-1})I_A \\ &+ I_B(w - H_B P_B G_B \mathbf{g}_B^{-1})I_B - IH_I I, \end{aligned} \quad (1)$$

where w represents the energy, $I = I_A + I_B$ is the interface complete projector, and P_M ($M = A, B$) is the projector of the semi-infinite crystal M . The coupling interaction across the interface is described by the last term of Eq. (1).

In order to obtain \mathbf{g}_I , the diagonal and nondiagonal elements of both A and B bulk GF matrices must be known. Their calculation requires, for each value of the energy, a cumbersome integration over those \mathbf{k} vectors which cover the projection of the bulk Brillouin zone (BZ) onto the surface. Nevertheless, the integration can be avoided by expressing Eq. (1) in terms of the transfer matrices T , \bar{T} , S , and \bar{S} ,²¹ which are defined as follows:

$$\begin{aligned} G_{n+1,m} &= TG_{nm}, \quad n \geq m \\ G_{n-1,m} &= \bar{T}G_{nm}, \quad n \leq m \\ G_{n,m+1} &= G_{nm}S, \quad m \geq n \\ G_{n,m-1} &= G_{nm}\bar{S}, \quad m \leq n; \end{aligned} \quad (2)$$

with these definitions, and since for the ideal interface the complete interface domain contains two principal layers, Eq. (1) can be written as

$$\mathbf{g}_I = \begin{bmatrix} (w - H_A)_{1,1} - H_{A;1,2}T_A & -H_{I;1,-1} \\ -H_{I;-1,1} & (w - H_B)_{-1,-1} - H_{B;-1,-2}T_B \end{bmatrix}^{-1}, \quad (3)$$

where the layer indexes denoted $1, 2, 3, \dots$ and $-1, -2, -3, \dots$ stand for the A and B semicrystal, respectively. To obtain the transfer matrices T and S , we have used a fast-convergence iterative procedure, developed by one of us,²³ which takes into account 2^n layers after n interactions. Once \mathbf{g}_I is known, the GF of any layer is obtained in terms of its own projection in the interface domain from the following expression:

$$G_{I;n,n} = G_{M;l,l} + T_M^{(n-1)}(g_{I;l,l} - G_{M;l,l})S_M^{(n-1)}, \quad (4)$$

where, for \mathbf{n} being on the A (B) side, l is equal to 1 (-1) and $M = A$ (B).

All the physics of the interface is contained in \mathbf{g}_I . Thus, the eigenvalues of the interface can be directly obtained from the secular equation:

$$\det|\mathbf{g}_I^{-1}(\mathbf{k}, w)| = 0, \quad (5)$$

and the layer density of states (LDOS) in the n th layer is given by

$$N_n(\mathbf{k}, w) = -(1/\pi) \lim_{\epsilon \rightarrow 0} \text{Im} \text{tr} G_{I;n,n}(\mathbf{k}, w + i\epsilon). \quad (6)$$

The \mathbf{k} -integrated LDOS's have been obtained by a weighted sum in the Cunningham special points of the two-dimensional BZ.²⁴

The geometry of the Cr/GaAs(001) interface is shown in Fig. 1(a). Because the bcc Cr lattice constant is almost a factor of 2 smaller than that of the zinc-blende-structure GaAs ($a_{\text{Cr}} \approx \frac{1}{2} a_{\text{GaAs}}$), the small lattice mismatch being neglected in this work, we assume that the (001) Cr atomic planes are placed at the same positions that the new (001) planes of GaAs would occupy if added. Thus, the distance between nearest-neighbor atoms at the interface coincides with the nearest-neighbor distance of both Cr and GaAs sublattices. Second-order interactions have been considered, but only among atoms placed at the second-neighbor distance of the bcc lattice. Since the number density of Cr atoms in a bcc (001) plane is twice that of GaAs, Cr atoms occupy both the lattice positions of the GaAs zinc-blende structure and the interstitial sites in the layer. Therefore, there are two chemically distinct Cr sites in each layer: the P Cr atoms that have a second-order neighbor at the second GaAs layer, and the M Cr atoms that do not. This distinction between the Cr lattice sites in each layer must be taken into account in the Hamiltonian equations, since the interactions with and between atoms placed at P and M sites differ. In Fig. 1(b) the geometrical structure of the (001) interface planes is represented schematically, and the two-dimensional unit cell is shown by the dashed line, the corresponding BZ being shown in Fig. 1(c). This BZ is actually that of the GaAs(001) surface, since it is

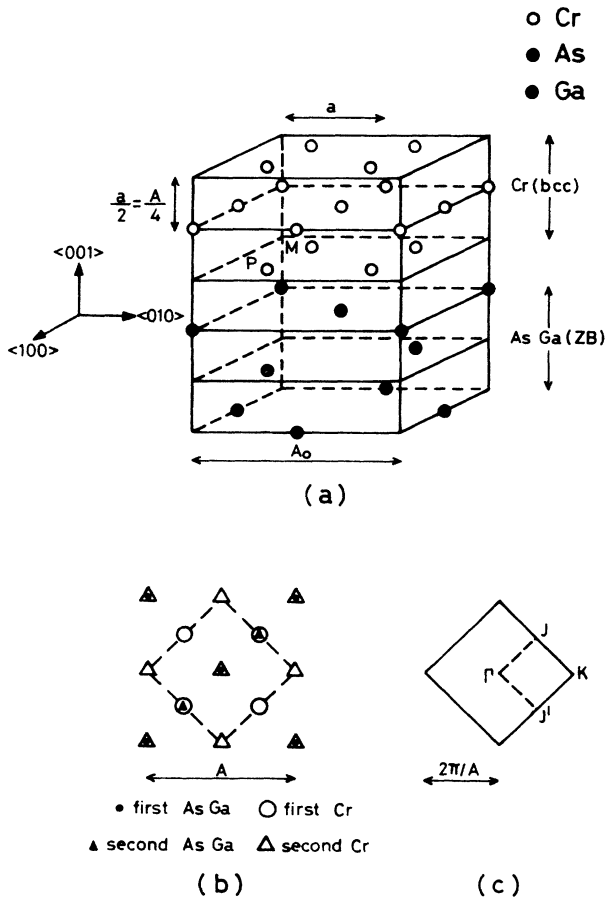


FIG. 1. (a) Schematic representation of a (001) interface of bcc Cr with (001) zinc-blende-structure GaAs. (b) Schematic geometrical structure of (001) planes of the Cr/GaAs interface; dashed line points out the unit cell. (c) Corresponding two-dimensional Brillouin zone.

inside the Cr(001) surface BZ, so the special points are labeled as in the zinc-blende structure.

The Slater-Koster²⁵ parametrized tight-binding scheme has been followed. For GaAs, a basis set consisting of $1s$ and $3p$ orbitals has been taken with only first-nearest-neighbor interactions; the parameters given by Chadi²⁶ have been used. This parametrization provides a good description of the valence band, although the conduction-band description is not so precise.²¹ For chromium only d states have been considered, since we are mainly interested in investigating how spin polarization affects the electronic structure. Therefore, at both the surface and the interface s and p Cr states are lacking. However, this approximation¹⁰ can be justified by the small contribution from delocalized s - and p -like electrons to both the surface LDOS and the magnetic moment²⁷ (see, for example, Table III and Figs. 3 and 5 in Ref. 13). Moreover, experimental results seem to point out that metal d states hybridize with the semiconductor p states to form the chemical bond in, i.e., Cr/GaAs,¹⁷ Cr/Si,²⁸ and Cr/Ge systems.²⁸ The TB parameters used

are those given by Allan.¹⁰ Both paramagnetic and antiferromagnetic states have been studied. In the antiferromagnetic case it is assumed that the spin wave is commensurate with the lattice spacing (actually, it is nearly commensurate^{10,27,29}), taking a spin wave vector $\mathbf{Q}=(2\pi/a_{\text{Cr}})(0,0,1)$. The (001) planes thus have alternately an up- or down-spin polarization, and the spin structure reduces the crystal symmetry. The antiferromagnetic crystal potential, in addition to the Coulomb terms as in the nonmagnetic case, has the exchange magnetic contribution $V_{\text{ex}}=\pm J\delta N_n$, where J is the effective intra-atomic exchange parameter adjusted in order to obtain the bulk experimental magnetization value of $0.59\mu_B/\text{atom}$, and $2\delta N_n$ represents the n -layer spin polarization. The plus or minus sign depends on the majority spin of the layer. The basis set for antiferromagnetic Cr is then formed by ten orbitals, five with spin-up polarization and five with spin-down polarization.

At the interface the matrix elements have been obtained as the geometric mean of the respective Cr and GaAs matrix elements. The sign of the greatest one, when the two elements have different sign, and the common sign, when they have equal sign, was chosen. This prescription was decided after some testing, which showed that the interface results were more sensitive to the matrix-element signs than to its absolute value. The choice of the geometric mean for the interface parameters has given good results for similar materials, for instance, two transition metals^{12,30} or two semiconductors.²¹ Moreover, calculations of the MnAs, CrAs, and FeAs electronic structure with a two-center TB model described, in good agreement with experiments, the general trend of the magnetic moments.³¹ In the calculations just referred to, the TB Hamiltonian consists of itinerant metal d states hybridized with nonmetal p states, and the pd parameters were obtained as the geometric mean of the elemental pp and dd matrix elements.

The Cr and GaAs Fermi levels were aligned at the interface and taken as the zero of energy. To obtain charge neutrality, we impose that the d -orbital occupancies at the surface and at the interface planes should not differ from the bulk values. For this reason we introduce a sort of potential in the diagonal matrix elements. This correction is due to changes not only in the diagonal terms (intra-atomic), but also in the nondiagonal matrix elements (interatomic). This type of approximation of the self-consistency has been proven to give reasonable results for TB Hamiltonians.^{10,12}

The matrices entering the interface calculation are 48×48 ; the GaAs Hamiltonian is an 8×8 matrix, with four orbitals per site, one atomic site, and one principal layer formed by two atomic planes. The Cr Hamiltonian is a 40×40 matrix since there are ten orbitals per atom, two different atomic sites, P and M , per layer, and two atomic layers enter in a principal layer. Despite the large size of the matrices for calculational purposes, the SGFM method has some advantages over other methods, since it provides an exact solution of \mathbf{g}_I , interface states can be unambiguously determined, and calculation of the LDOS at any desired layer on both semicrystals is allowed.

III. RESULTS

A. Cr(001) surface

Both experimental^{11,32-36} and theoretical work^{10,12,13,37-46} devoted to the study of the Cr(001) surface has shown that this surface possesses peculiar magnetic properties: surface ferromagnetism while retaining an antiferromagnetic ground state in the bulk, and a great enhancement of the surface magnetic moment with respect to the bulk value. Since a by-product of the interface calculation is the surface-electronic properties,^{21,22} the electronic structure of both paramagnetic and antiferromagnetic Cr(001) surfaces are presented. Figure 2(a) shows the LDOS for the first six atomic layers and a bulk plane in the paramagnetic state. Diagonal corrections of 0.136 and 0.125 eV in the first and second layer, respectively, were necessary in order to achieve charge neutrality at the surface. As can be observed in Fig. 2(a), the peak which appears at about 1 eV below E_F in the surface DOS is completely localized in the first atomic layer, and only small differences exist between the next interior plane DOS's and that of the bulk plane.

In the antiferromagnetic state, self-consistency was attained by varying the surface magnetic potential. Charge neutrality, to within 0.01 electron, was obtained for 0.9- and 0.7-eV surface magnetic potentials at the first and second layers, respectively. The resulting spin-up and spin-down LDOS's for the first six atomic layers and a bulk plane are presented in Fig. 2(b). As expected, and in

agreement with previous calculations,¹⁰ both bulk spin-up and spin-down LDOS's are close and similar to the corresponding bulk LDOS's of paramagnetic chromium. The surface LDOS's are completely different, while the spin-up LDOS is mainly formed of occupied states, the unoccupied-state area is predominant in the spin-down LDOS. This imbalance of spin-up and spin-down states explains the enhancement of the magnetic moment in the surface region. A surface magnetic moment of $2.79\mu_B$ is obtained, in agreement with earlier calculations [$2.8\mu_B$,¹⁰ $3\mu_B$,¹² and $2.49\mu_B$ (Ref. 13)]. However, the spin polarization of the next interior planes, instead of quickly approaching the bulk value (Ref. 12 gives, for the second to sixth layers, $-1.56\mu_B$, $1.0\mu_B$, $-0.93\mu_B$, $0.86\mu_B$, and $-0.85\mu_B$, respectively, and Ref. 13, gives for the second, third and center layers, $-1.29\mu_B$, $0.89\mu_B$, and $-0.89\mu_B$, respectively), shows a slow tendency to approach it, $-2.26\mu_B$, $2.43\mu_B$, $-2.33\mu_B$, $2.12\mu_B$, and $-2.03\mu_B$, and only at the twelfth layer is the $0.56\mu_B$ bulk magnetic moment reached.

The slow decay of the surface spin polarization to the bulk value could be related to the size of the surface magnetic potentials used to obtain charge neutrality, since for a value of 0.6 eV at the first two layers the bulk spin polarization was reached at the fourth layer, but a charge transfer of 0.3 electrons was found. Although the surface magnetic potentials seem very large if compared with the 0.2-eV bulk magnetic contribution, adjusted to obtain the $0.56\mu_B$ experimental magnetization, they are similar to

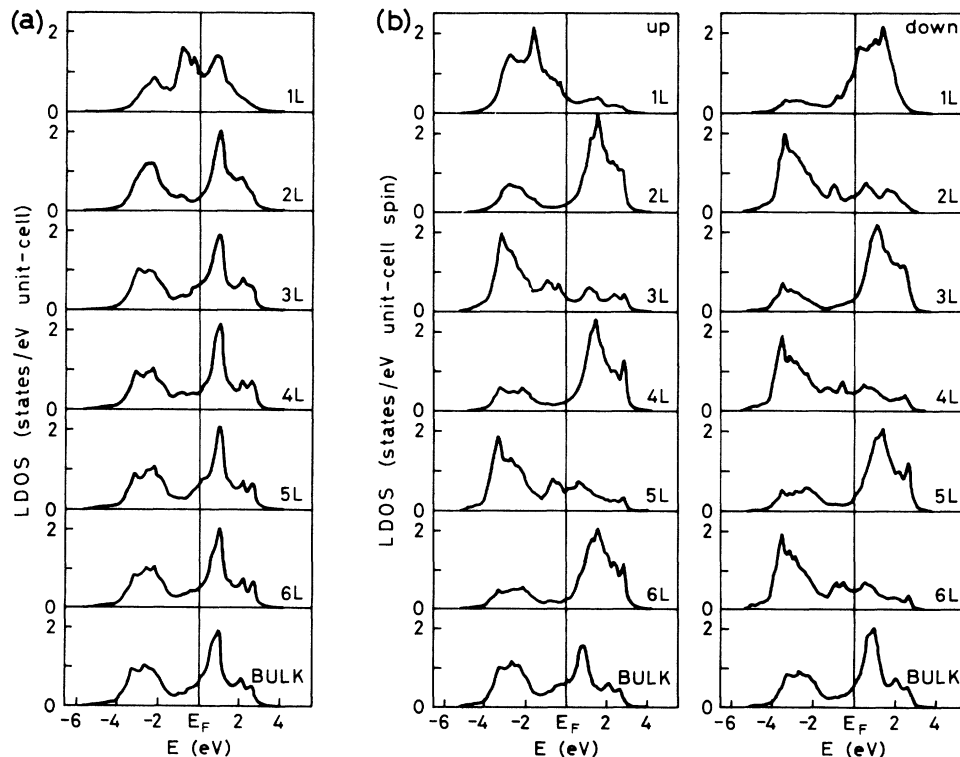


FIG. 2. Total LDOS for the (001) Cr surface, for the next four interior layers and for a bulk layer: (a) paramagnetic chromium and (b) antiferromagnetic chromium.

the only available datum, 0.9 eV, reported by Allan.¹⁰ However, in Allan's calculation it was assumed that the spin polarization retains the bulk value, except in the surface plane, so the magnetic moment decay length obtained here cannot be directly compared. Moreover, 0.9 and 0.7 eV are in agreement with the 0.8-eV surface magnetic gap estimated from the temperature dependence of the splitting of the surface resonance state in angle resolved photoemission spectroscopy (ARPES).¹³ We would like to point out that these numbers correspond not only to magnetic corrections due to the surface, but also to variations of the intra-atomic and interatomic Coulomb interactions. The last contribution would give rise to a surface dipole potential, but any estimation of its absolute value is not within the scope of the TB approximation. A fully-self-consistent calculation would be necessary to treat the dipole effects properly. However, TB self-consistent calculations for semiconductor interfaces with diagonal corrections greater than 0.5 eV properly described the electronic properties of the interfaces.⁴⁷ Since *s* and *p* electrons are not taken into account, there is no claim to quantitative accuracy, because the *s-p* hybridization can slightly distort the calculated DOS. Nevertheless, the large spin polarization of the layers near the surface could explain the absence of detectable magnetization in spin-resolved photoemission experiments,³⁴ without invoking the existence of terraces.⁴⁶ In fact, the thickness of the surface layer probed in Ref. 34 is about 20 Å, equivalent to 13 or 14 atomic planes.

The surface-projected band structure (PBS), along the high-symmetry directions of the Cr(001) two-dimensional BZ [note that the Cr(001) surface BZ is twice as large as the interface BZ depicted in Fig. 1 (c)], has been plotted in Fig. 3 for both spin-up and spin-down polarizations. The PBS gives information on all the gaps and pockets in which true surface states (SS's) can exist, thus allowing us to identify the *bona fide* SS's unambiguously. In Fig. 3 the SS's are denoted by +', while the limits of continuum regions are indicated by ●'s. A large absolute gap along the *MX* direction, in both spin-up and spin-down PBS's, is obtained with two and one occupied SS, respectively. These SS's have binding energies lower than 2 eV below E_F . Small gaps along the ΓM direction also appear, although no gaps are found along the ΓX direction. However, in the ΓX direction many surface resonances (SR's) are developed, although for the sake of clarity the SR's are not plotted in the figure.

In Fig. 4 the LDOS at the Γ point of the surface Brillouin zone (SBZ) is shown for both surface and bulk atomic planes. In order to see the total change induced by the surface, the difference between surface and bulk atomic planes is represented at the bottom. The features of both spin-up and spin-down difference spectra can be identified as resonances and antiresonances; both being balanced, the number of states is conserved and Levinson's theorem is satisfied. The spin-up difference spectrum is dominated by two peaks at 3.5 and 1.5 eV which we identify as SR's, since no absolute gap were found at the Γ point. These values are slightly higher than the 3.25 and 1.35 eV obtained in slab calculations.¹¹ The lower-binding-energy (1.5 eV) SR may correspond to

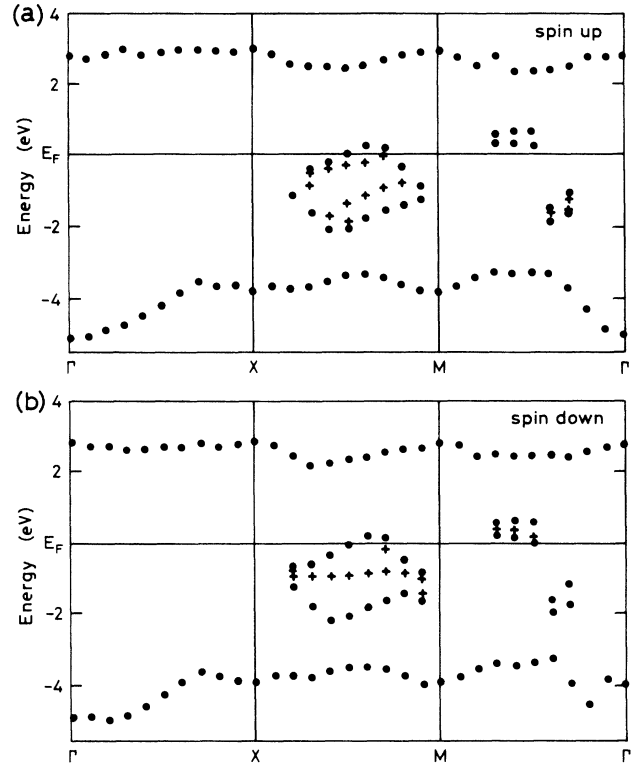


FIG. 3. Surface-protected band structure of the (001) Cr surface along the high-symmetry directions of the bcc two-dimensional Brillouin zone: (a) for spin-up states and (b) for spin-down states.

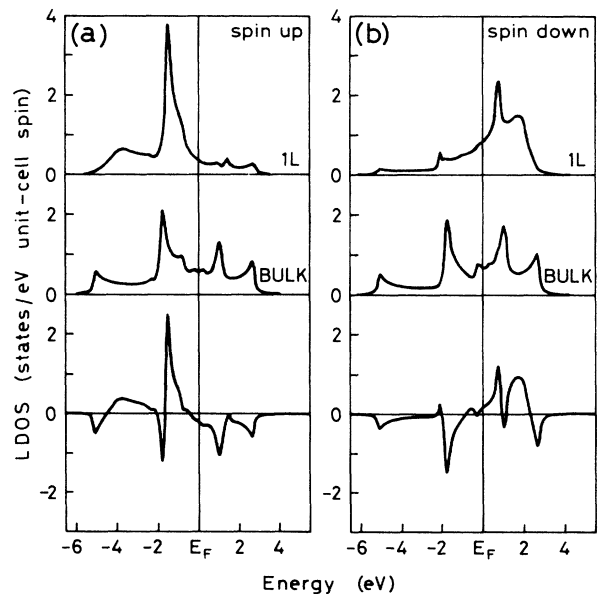


FIG. 4. Local density of states at the Γ point of the two-dimensional BZ for the (001) Cr surface, for a bulk plane and their difference: (a) spin-up states and (b) spin-down states.

the 0.75-eV state measured at 300 K by normal-emission ARPES,³² taking into account that the *s* and *p* bands have not been included. The spin-down difference spectrum has a very low LDOS for energies below E_F and only a small SR at about 2.5 eV appears.

B. Cr/GaAs(001) interface

The LDOS's for the first four atomic planes on each side of the Cr-Ga and Cr-As interfaces are presented in Figs. 5–8. Figures 5 and 7 correspond to the spin-up Cr DOS and Figs. 6 and 8 to the spin-down Cr DOS. The Cr DOS's plotted in the four figures are those of atoms placed at *P* sites. The differences between the DOS's of *P* and *M* atoms are indicated as thinner lines, being only significant in the first two interface atomic planes. The general structure of the two ideal interface LDOS's is similar. Both LDOS's show a significant amount of interface-induced effects and show analogous evolution at the metal and semiconductor sides of the geometrical in-

terface. The changes induced in the LDOS are mainly restricted to the first atomic plane in the Cr semicrystal, while the interface LDOS decays more slowly to the bulk shape on the GaAs side. Then, the induced effects extend for at least two layers further in GaAs than in Cr, as is expected from the localized character of the *d* orbitals. This behavior is observed in both spin polarizations. On the semiconductor side, a large DOS appears in the fundamental gap up to three atomic planes. Then, metal-induced gap states occur and are responsible for the metallic character of both Cr-Ga and Cr-As interfaces. Interface perturbation is not restricted to the energy gap; rather it covers the entire energy range of the Cr bandwidth. Furthermore, changes of the DOS with respect to the bulk DOS are observed in both valence and conduction bands at energies for which the Cr LDOS is very small; see, for example, the structure around -6 eV in the Cr-Ga interface or the sharp peak around -10 eV in the Cr-As interface.

On the Cr side, beyond the first atomic plane both spin-up and spin-down LDOS's are similar to the bulk DOS. The main interface-induced states are restricted to the first layer and primarily near the Fermi level. The shape of the Cr DOS curves resembles rather a Cr surface

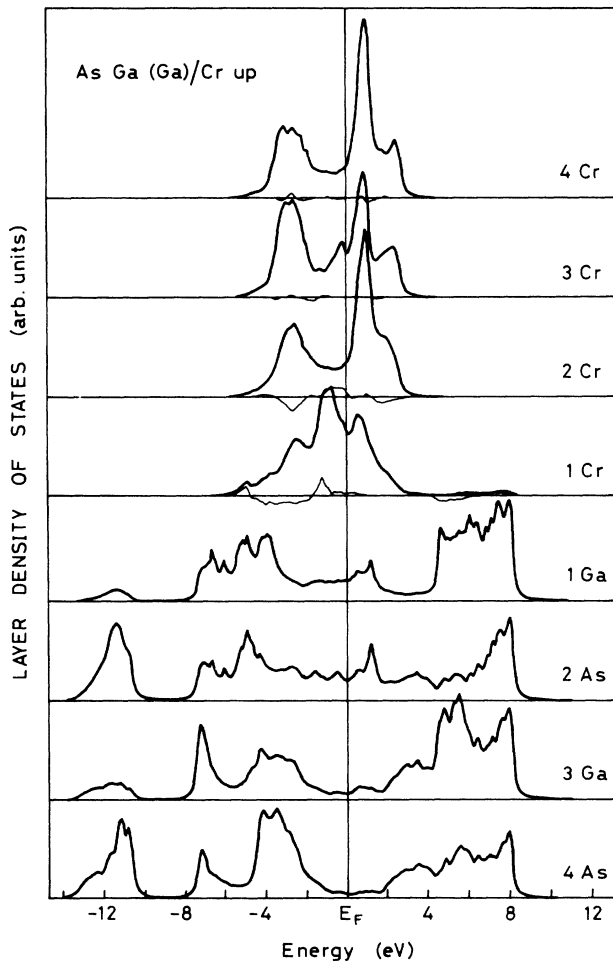


FIG. 5. LDOS integrated over the two-dimensional BZ for the first four atomic planes on each side of the Cr-Ga interface, for spin-up states corresponding to the lattice site denoted *P*. Thin lines on the Cr layers indicate the difference between the LDOS's of the *P* and *M* Cr sites.

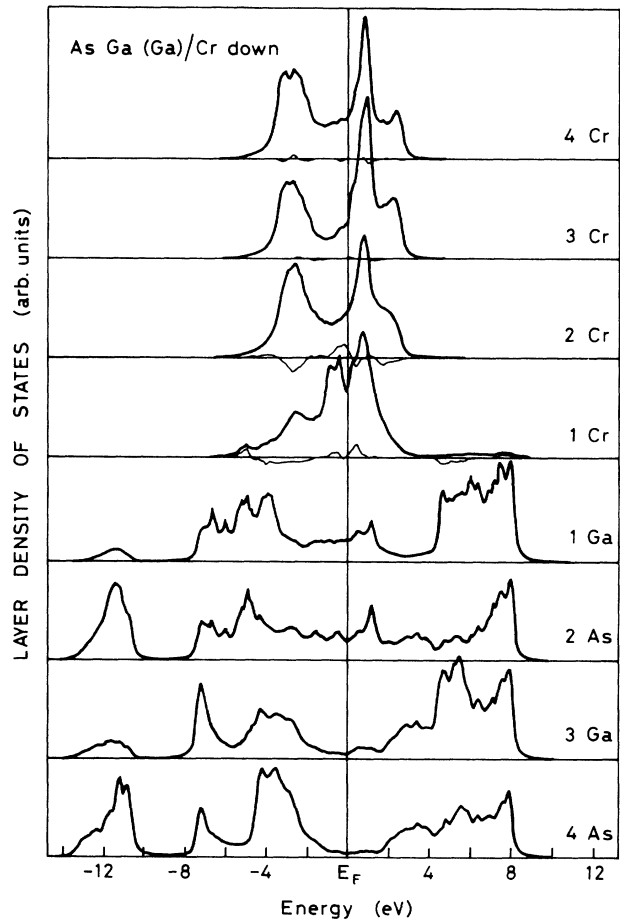


FIG. 6. As in Fig. 5, but for spin-down states.

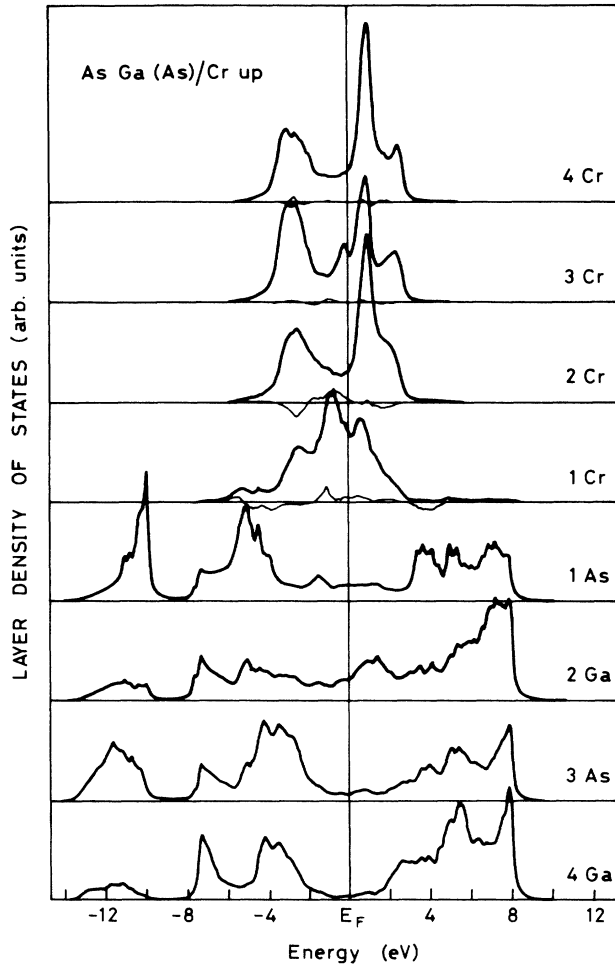


FIG. 7. As in Fig. 5, but for the Cr-As interface.

DOS than it does a DOS of the bulk. This must be due to the fact that Cr atoms at the interface have occupied only half of their first-nearest-neighboring sites on the Ga(As) first layer. However, due to GaAs-Cr hybridization, the first-layer Cr DOS extends to a larger energy region than those of the (001) surface, or even of the bulk Cr DOS.

In the interface calculations charge neutrality was achieved by shifting the on-site energies of atoms near the interface. For the Cr-Ga interface a charge transfer of 0.01 electron has been obtained, shifting the on-site energies of the Cr interface atoms by 0.1 eV, which seems a sufficiently good result. The magnetic moment is $0.76\mu_B$, slightly greater than the bulk magnetic moment of chromium. For the Cr-As interface the charge transfer is greater, 0.02 electron, and the magnetic moment obtained is $0.79\mu_B$. In absence of experimental evidence, spin polarization of the GaAs has not been allowed. However, it is possible that, as in the Cr/Au(001) interface,⁴² a small magnetic moment may be induced onto the GaAs interface layer.

Nevertheless, further penetration into the bulk is not probable, as in the Cr/Au (Ref. 42) and Fe/Ge (Ref. 5) systems, where no spin polarization is found on the plane

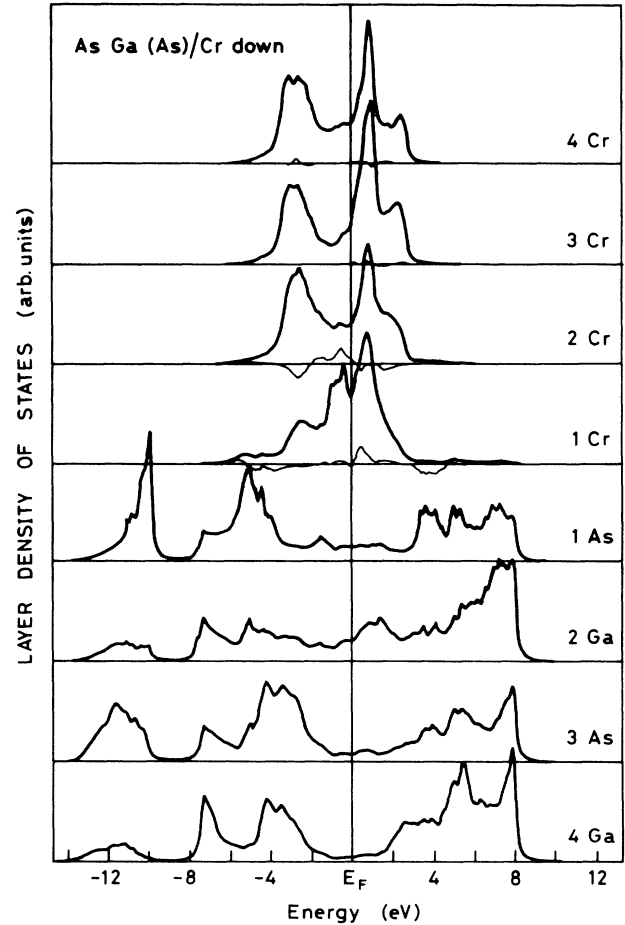


FIG. 8. As in Fig. 6, but for the Cr-As interface.

next to the interface. The present results show an enhancement of the Cr magnetic moment at the interface with respect to its bulk value, but much lower than that produced at the free surface, so the magnetic proximity effect is larger in the Cr/GaAs interface than in Cr-noble-metal interfaces.⁴²

IV. CONCLUSIONS

The (001) interfaces of Cr/GaAs are found to be of a metallic character. The main changes appear in the energy range from -6 to 6 eV (which coincides with the Cr *d*-band width), especially around the Fermi level, where the DOS increases in both chromium and gallium arsenide. Interface-induced effects in the LDOS are significant in the first two layers on the semiconductor side, and in the first Cr atomic plane. Density of states is found in the GaAs gap at both interfaces, which extends three layers further into the semiconductor. The magnetic moment of a Cr atom at the interface, although higher than at a bulk atom, is considerably lower than at the (001) surface due to the presence of the GaAs overlayers.⁴⁸

- ¹W. A. Harrison, *Electronic Structure and the Properties of Solids* (Freeman, San Francisco, 1980).
- ²L. J. Brillson, *Surf. Sci. Rep.* **2**, 123 (1982).
- ³G. Le Lay, *Surf. Sci.* **132**, 169 (1983).
- ⁴S. M. Sze, *Physics of Semiconductor Devices* (Wiley-Interscience, New York, 1981).
- ⁵W. E. Pickett and D. A. Papaconstantopoulos, *Phys. Rev. B* **34**, 8372 (1986).
- ⁶T. G. Andersson, J. Kanski, G. Le Lay, and S. P. Svensson, *Surf. Sci.* **168**, 301 (1986).
- ⁷M. del Giudice, M. Grioni, J. J. Joyce, M. W. Ruckman, S. A. Chambers, and J. H. Weaver, *Surf. Sci.* **168**, 309 (1986).
- ⁸G. Hughes, R. Ludeke, F. Schaffler, and D. Rieger, *J. Vac. Sci. Technol. B* **4**, 924 (1986).
- ⁹N. Newman, W. E. Spicer, T. Kendelewicz, and I. Lindau, *J. Vac. Sci. Technol. B* **4**, 931 (1986).
- ¹⁰G. Allan, *Surf. Sci.* **74**, 79 (1978).
- ¹¹L. E. Klebanoff, R. H. Victora, L. M. Falicov, and D. A. Shirley, *Phys. Rev. B* **32**, 1997 (1985).
- ¹²R. H. Victora and L. M. Falicov, *Phys. Rev. B* **31**, 7335 (1985).
- ¹³C. L. Fu and A. J. Freeman, *Phys. Rev. B* **33**, 1755 (1986).
- ¹⁴M. W. Ruckman, M. del Giudice, J. J. Joyce, and J. H. Weaver, *Phys. Rev. B* **33**, 8039 (1986).
- ¹⁵T. Zeng-ju, C. Satoko, and S. Ohnishi, *Phys. Rev. B* **36**, 6390 (1987).
- ¹⁶A. Franciosi, J. H. Weaver, D. G. O'Neill, F. A. Schmidt, O. Bisi, and C. Calandra, *Phys. Rev. B* **28**, 7000 (1983).
- ¹⁷J. H. Weaver, M. Grioni, and J. Joyce, *Phys. Rev. B* **31**, 5348 (1985).
- ¹⁸F. Xu, Z. Lin, D. M. Hill, and J. H. Weaver, *Phys. Rev. B* **36**, 6624 (1987).
- ¹⁹C. L. Fu and A. J. Freeman, *Phys. Rev. B* **33**, 1611 (1986); M. B. Brodsky, P. Marikar, R. J. Friddle, L. Singer, and C. H. Sowers, *Solid State Commun.* **42**, 675 (1982).
- ²⁰F. Garcia-Moliner and V. R. Velasco, in *Progress in Surface Science*, edited by S. G. Davidson (Academic, New York, 1986), Vol. 21, p. 93.
- ²¹M. C. Muñoz, V. R. Velasco, and F. Garcia-Moliner, *Phys. Scr.* **35**, 504 (1987); in *Progress in Surface Science*, edited by S. G. Davidson (Academic, New York, 1987), Vol. 26, p. 117.
- ²²M. C. Muñoz, V. R. Velasco, and F. Garcia-Moliner, *Phys. Rev. B* **39**, 1786 (1989).
- ²³M. P. López Sancho, J. M. López Sancho, and J. Rubio, *J. Phys. F* **14**, 1205 (1984); **15**, 851 (1985).
- ²⁴S. L. Cunningham, *Phys. Rev. B* **10**, 4988 (1974).
- ²⁵J. C. Slater and G. F. Koster, *Phys. Rev.* **94**, 1498 (1954).
- ²⁶D. J. Chadi, *Phys. Rev. B* **16**, 790 (1977).
- ²⁷J. Friedel, in *Physics of Metals*, edited by J. Ziman (Cambridge University Press, Cambridge, 1969), pp. 340–408.
- ²⁸A. Franciosi, D. J. Peterman, J. H. Weaver, and V. L. Moruzzi, *Phys. Rev. B* **25**, 4981 (1982).
- ²⁹C. R. Fincher, G. Shirane, and S. A. Werner, *Phys. Rev. Lett.* **43**, 1441 (1979).
- ³⁰T. Thyma, Y. Ohta, and M. Shimizu, *J. Phys. Condens. Matter* **1**, 1789 (1989).
- ³¹R. Podloucky, *J. Magn. Magn. Mater.* **43**, 204 (1984); **43**, 291 (1984).
- ³²L. E. Klebanoff, S. W. Robey, G. Liu, and D. A. Shirley, *Phys. Rev. B* **30**, 1048 (1984).
- ³³C. Rau and S. Eichner, *Phys. Rev. Lett.* **47**, 939 (1981).
- ³⁴F. Meier, D. Pescia, and T. Schriber, *Phys. Rev. Lett.* **48**, 645 (1982).
- ³⁵A. A. Aligia, J. Dorantes-Dávila, J. L. Morán-López, and K. H. Bennemann, *Phys. Rev. B* **35**, 7053 (1987).
- ³⁶S. Raaen and V. Murgai, *Phys. Rev. B* **36**, 887 (1987).
- ³⁷S. Asano and J. Yamashita, *J. Phys. Soc. Jpn.* **23**, 714 (1967).
- ³⁸D. R. Grempel, *Phys. Rev. B* **24**, 3928 (1981).
- ³⁹D. G. Laurent, J. Callaway, J. L. Fry, and N. E. Brener, *Phys. Rev. B* **23**, 4977 (1981).
- ⁴⁰J. Xu, A. J. Freeman, T. Jarlborg, and M. B. Brodsky, *Phys. Rev. B* **29**, 1250 (1984).
- ⁴¹P. J. Feibelman and D. R. Hamann, *Phys. Rev. B* **31**, 1154 (1985).
- ⁴²C. L. Fu and A. J. Freeman, *J. Magn. Magn. Mater.* **54-57**, 777 (1986).
- ⁴³N. I. Kulikov, M. Alouani, M. A. Khan, and M. V. Magnitskaya, *Phys. Rev. B* **36**, 929 (1987).
- ⁴⁴A. J. Freeman and C. L. Fu, *J. Appl. Phys.* **61**, 3356 (1987).
- ⁴⁵S. Blügel, M. Weinert, and P. H. Dederichs, *Phys. Rev. Lett.* **60**, 1077 (1988).
- ⁴⁶S. Blügel, D. Pescia, and P. H. Dederichs, *Phys. Rev. B* **39**, 1392 (1989).
- ⁴⁷G. Platero, J. Sánchez-Dehesa, C. Tejedor, F. Flores, and A. Muñoz, *Surf. Sci.* **172**, 47 (1986).
- ⁴⁸L. M. Falicov, R. H. Victora, and J. Tersoff, in *The Structure of Surfaces*, Vol. 2 of *Springer Series in Surface Science*, edited by M. A. Van Hove and S. Y. Tong (Springer-Verlag, Berlin, 1985), p. 12.